The Canadian Mineralogist
Vol. 41, pp. 1125-1134 (2003)

MÖSSBAUER STUDY OF Fe-BEARING SYNTHETIC TENNANTITE

Emil MAKOVICKY[§]

Geologisk Institut, Københavns Universitet, Øster Voldgade 10, DK–1350 København K, Denmark

Gerold TIPPELT, Karl FORCHER and Werner LOTTERMOSER

Institut für Mineralogie, Universität Salzburg, Hellbrunnerstrasse 34, A–5020 Salzburg, Austria

Sven KARUP-MØLLER

Institut for Miljø og Ressourcer, Danmarks Tekniske Universitet, DK–2800 Kongens, Lyngby, Denmark

Georg AMTHAUER

Institut für Mineralogie, Universität Salzburg, Hellbrunnerstrasse 34, A–5020 Salzburg, Austria

Abstract

The valence of iron in synthetic Fe-bearing tennantite was investigated by the Mössbauer method. Tennantite compositions were weighed out in the reference system $Cu_{12}As_4S_{13}$ – $Cu_{14}As_4S_{13}$ – $Cu_{10}Fe_2As_4S_{13}$ at the levels with 0.0, 0.5, 1.0, 1.5 and 1.7 Fe *apfu*. The tennantite compositions obtained were characterized by electron-microprobe analysis and powder-diffraction data. Compositions with a low-level substitution of iron for copper contain Fe^{3+}. Evidence of divalent iron appears at the level of 1.0 Fe *apfu*, and for Cu-rich charges, even at 0.5 Fe *apfu*. It becomes dominant in Cu-rich tennantite at ~1.0 Fe *apfu*, whereas in Cu-poor tennantite, only at ~1.4 Fe *apfu*. The balance of the iron is in both cases represented by mixed-valence iron, with the values of isomer-shift and quadrupole splitting intermediate between those for Fe^{2+} and Fe^{3+}. Effects of electron delocalization and net charge-transfer in superexchange interactions on the effective valence of iron were modeled using the relation between isomer shift and valence proposed by Goodenough & Fatseas for sulfides.

Keywords: Fe-bearing tennantite, Mössbauer study, valence of iron, mixed-valence iron.

Sommaire

Nous avons étudié la valence du fer dans la tennantite ferrifère synthétique par spectroscopie de Mössbauer. Les compositions de tennatite contenant 0.0, 0.5, 1.0, 1.5 et 1.7 atomes de fer par unité formulaire (*apuf*) ont été préparées par référence au système $Cu_{12}As_4S_{13}$ – $Cu_{14}As_4S_{13}$ – $Cu_{10}Fe_2As_4S_{13}$. Nous avons caractérisé ces compositions par analyse à la microsonde électronique et par diffraction X (méthode des poudres). Les compositions ayant une faible teneur en fer, en substitution au cuivre, contiennent le fer sous forme Fe^{3+}. Des signes de la présence de Fe^{2+} sont décelables dans les compositions contenant 1.0 Fe *apuf*, et dans les compositions riches en Cu, même à 0.5 Fe *apuf*. Il devient prédominant dans la tennantite riche en Cu à environ 1.0 Fe *apuf*, tandis que dans la tennantite à faible teneur en Cu, seulement à ~1.4 Fe *apuf*. Le reste du fer dans les deux cas serait représenté par le fer à valence mixte, les valeurs de la dédoublure isomère et de la séparation quadrupolaire sont intermédiaires entre ceux du Fe^{2+} et du Fe^{3+}. Les effets qu'ont la délocalisation des électrons et le transfert net des charges dans les interactions de type super-échange sur la valence effective du fer ont été reconstruits en adoptant la relation entre la dédoublure isomère et la valence qu'avait proposé Goodenough et Fatseas pour les sulfures.

(Traduit par la Rédaction)

Mots-clés: tennantite ferrifère, spectroscopie de Mössbauer, valence du fer, fer de valence mixte.

[§] *E-mail address*: emilm@geol.ku.dk

INTRODUCTION

Tennantite is the arsenic end-member of the multiparameter tetrahedrite–tennantite solid solution. The pure copper end-member, tennantite, ideally $Cu_{12}As_4S_{13}$, has been repeatedly synthesized, and shows a slight excess in Cu; a solid solution, $Cu_{12+x}As_4S_{13}$ stretching at least to the composition $Cu_{13.7}Sb_4S_{13}$, has been established by Maske & Skinner (1971). However, the majority of natural As-rich members of the solid solution comply with the formula $(Cu,Ag)_{10}(Fe,Zn,Cu,...)_2(As,Sb)_4S_{13}$. Silver contents being generally low in natural tennantite, iron is the most important minor element in the mineral, in association with Zn (Charlat & Lévy 1975, Mozgova & Tsepin 1983, Johnson *et al.* 1988). An experimental study of the compositional field of Fe-bearing tennantite in the system Cu–Fe–As–S was carried out by Bortnikov & Nekrasov (1987).

Since the first Mössbauer studies of tetrahedrite by Kawai *et al.* (1972) and Vaughan & Burns (1972), Mössbauer spectroscopy has been found useful in studies of the tetrahedrite–tennantite series, with special emphasis on the Sb-rich end-members (Charnock *et al.* 1989a, b, Makovicky *et al.* 1990). This study is a sequel to our study of Fe-bearing tetrahedrite (Makovicky *et al.* 1990, Makovicky & Karup-Møller 1994).

Inspection of the shape of the composition volume of synthetic Fe-bearing tennantite solid-solution in the composition space Cu–Fe–As–S obtained by Bortnikov & Nekrasov (1987) suggested to us that the situation for tennantite differs from that observed by Tatsuka & Morimoto (1977) and re-investigated by Makovicky & Karup-Møller (1994) for Fe-bearing tetrahedrite. Further incitement to this study were the results of Charnock *et al.* (1989a, b) on the only sample of tennantite included in their Mössbauer study of tetrahedrite, which showed a valence of iron inconsistent with the models derived for tetrahedrite by them and Makovicky *et al.* (1990).

EXPERIMENTAL

Samples of synthetic tennantite were prepared as 500 mg charges in evacuated silica glass tubes from analytical-grade pure elements. They were annealed for six weeks at 450°C, interrupted by one step of regrinding and homogenization. After quenching, the charges were examined by reflected-light microscopy and analyzed with an electron microprobe, as well as with Guinier diffractograms obtained from powdered samples. A JEOL Superprobe 733 was used in wavelength-dispersion mode, with on-line correction programs supplied by JEOL. Synthetic Cu_3AsS_4 and natural FeS served as standards. Guinier patterns obtained with Cu$K\alpha$ radiation and quartz as an internal standard were used for phase analysis of reaction products and determination of the unit-cell parameter *a* of tennantite from a set of selected diffraction lines.

Mössbauer spectroscopy was performed using a constant-acceleration spectrometer (Halder Elektronik GmbH) with a multichannel analyzer (1024 channels) in conjunction with an electromechanical drive system with a symmetrical triangular shape of velocity distribution. All ^{57}Fe spectra were recorded with a source of 25 or 50 mCi ^{57}Co in a Rh matrix at room temperature. The powdered samples were prepared as a Mössbauer absorber with a maximal concentration of 5 mg Fe/cm^2 and a diameter of either 7 or 10 mm, by embedding the sample homogeneously in an epoxy glue with good thermal conductivity, and fixing it in a copper ring. The velocity scale of the spectrometer was calibrated with an α-Fe foil. In order to improve statistics, the two symmetrical spectra obtained were folded to 510 channels. For a good resolution and a good peak-to-background ratio, high count-rates of generally more than 1 million were chosen. For the fitting procedure, we used the program MOESALZ from Lottermoser *et al.* (1993). The Mössbauer spectra were evaluated with quadruple doublets, assuming a Lorentzian shape of the lines. In some of the fits, we had to use a fixed value for FHWB in order to get a stable solution.

The analyzed charges were weighed out as tennantite compositions in the reference triangle $Cu_{12}As_4S_{13}$ – $Cu_{14}As_4S_{13}$ – $Cu_{10}Fe_2As_4S_{13}$ at the levels with 0.0, 0.5, 1.0, 1.5 and 2.0 Fe *apfu*. This approach was used because according to Maske & Skinner (1971), the range of *y* values in the solid-solution field $Cu_{12+x}As_{4+y}S_{13}$ is small, $0 \leq y \leq 0.08$. Charge compositions, results of electron-microprobe analyses, unit-cell parameters, data on trace amounts of other phases present in some charges, and final estimates of composition for the tennantite synthesized are summarized in Table 1. Mössbauer spectroscopy data are compiled in Table 2.

Electron-microprobe analyses of tetrahedrite with less than two atoms of minor elements (such as Fe, Zn and Hg) in a formula unit are plagued by analytical problems specific to these compounds. As discovered by Lind & Makovicky (1982) for the case of substitution-free tetrahedrite and corroborated in detail by Makovicky & Karup-Møller (1994) for partly substituted tetrahedrite, all Cu in excess of 12 metal atoms (*Me* = Cu, Zn, Fe,...) in a formula unit based on 13 sulfur atoms remains undetected in electron-microprobe analyses, probably as a result of the ionic conductor nature of tetrahedrite with excess copper (Makovicky & Skinner 1979). What is important for the present study is that the same phenomenon was observed by Bortnikov & Nekrasov (1987) for synthetic Fe-containing tennantite.

Therefore, final estimates of composition for the phases studied (Table 1) were obtained by evaluating critically the initial compositions of the charges, the yield of tennantite in them, the nature of minor phases present, the electron-microprobe data, and values of the unit-cell parameter. Results of such a combined approach applied to a broad range of partly substituted synthetic tetrahedrite compositions containing Fe, Zn,

TABLE 1. ANALYTICAL DATA ON SYNTHETIC Fe-SUBSTITUTED TENNANTITE

Charge No.	Phase	Volume %	*n*	As wt%	Cu wt%	Fe wt%	S wt%	Total wt%	As *apfu*	Cu *apfu*	Fe *apfu*	S *apfu*	*a* Å
2052	Tn	98	12	20.36(25)	49.39(32)	2.18(21)	28.84(37)	100.89	3.93	11.24	0.57	13.00	10.174(8)
	Luz	2	n.a.										
	Charge composition								4.00	11.5	0.5	13.0	
	Estimate of final composition								4.00	11.44	0.58	13.0	
2053	Tn	95	10	20.22(24)	51.86(25)	0.01(1)	28.76(73)	100.85	3.91	11.83	0.00	13.00	10.168(7)
	Luz	5	n.a.										
	Charge composition								4.00	12.0	0.0	13.0	
	Estimate of final composition								4.0	12.10	0.0	13.0	
2054	Tn	100	11	20.32(26)	47.73(16)	4.02(12)	28.50(23)	100.57	3.96	10.99	1.05	13.00	10.194(7)
	Charge composition								4.0	11.0	1.0	13.0	
	Estimate of final composition								4.00	10.95	1.05	13.0	
2055	Tn	92	5	20.66(20)	45.92(26)	5.38(5)	28.59(18)	100.55	4.02	10.54	1.41	13.00	10.197(8)
	Cp	4	1	0.4	34.24	31.43	35.03	100.74	0.01	6.41	6.70	13.00	
	Bn	4	1	0.04	61.15	12.66	26.46	100.31	0.01	15.16	3.57	13.00	
	Charge composition								4.00	10.50	1.50	13.0	
	Estimate of final composition								4.00	10.59	1.41	13.0	
2056	Tn	85	12	20.26(24)	44.77(30)	6.46(14)	28.79(42)	100.28	3.91	10.20	1.67	13.00	10.205(4)
	Cp, Bn	≤15	n.a.										
	Charge composition								4.0	10.0	2.0	13.0	
	Estimate of final composition								4.0	10.30	1.70	13.00	
2057	Tn	100	11	20.06(43)	48.22(87)	3.98(7)	28.33(60)	100.59	3.94	11.16	1.04	13.00	10.212(5)
	Charge composition								4.0	12.0	1.0	13.0	
	Estimate of final composition								4.00	11.53	1.05	13.00	
2058	Tn	>95	11	19.34(22)	50.91(44)	1.94(3)	27.98(27)	100.17	3.84	11.94	0.51	13.00	10.212(5)
								i.e.	4.00	12.44	0.53	13.54	
	Luz	<5	n.a.										
	Charge composition								4.0	13.0	0.50	13.00	
	Estimate of final composition								4.00	12.73	0.53	13.00	
2059	Tn	93	15	20.29(24)	45.50(25)	5.79(7)	29.04(36)	100.62	3.88	10.27	1.48	13.00	10.209(29)
								i.e.	4.00	10.59	1.53	13.40	
	Bn	~7	n.a.										
	Charge composition								4.0	11.0	1.5	13.0	
	Estimate of final composition								4.0	10.98	1.50	13.00	

Symbols: Tn tennantite, Luz luzonite, Cp chalcopyrite, Bn bornite, *n*: number of points analyzed, *apfu*: atoms per formula unit, n.a.: not analyzed.

Ni, Co and Mn can be found in Makovicky & Karup-Møller (1994).

RESULTS

If we assume that the excess Cu over 12 metal atoms per formula unit causes the same change in unit-cell parameter for all regions of the $Cu_{12}As_4S_{13}$ – $Cu_{10}Fe_2As_4S_{13}$ – $Cu_{14}As_4S_{13}$ system, we can derive the composition of a Cu-rich sample from its *a* value. The Cu-poor samples are assumed to be positioned on the $Cu_{12}As_4S_{13}$ – $Cu_{10}Fe_2As_4S_{13}$ line, as weighed in.

From the study of Maske & Skinner (1971), the unit-cell parameter *a* of $Cu_{12}As_4S_{13}$ can be obtained by extrapolation as 10.160 Å, whereas that of $Cu_{14}As_4S_{13}$ is inferred to be 10.222 Å, *i.e.*, we obtain $\Delta a = 0.062$ Å for a difference of 2 Cu atoms per formula unit (*apfu*). Applying this incremental change in the *a* parameter to the 0.5 Fe *apfu* level, sample 2058 ought to have 1.26 more Cu *apfu* than sample 2052, which was estimated to be $Cu_{11.44}Fe_{0.58}As_4S_{13}$ (Table 1). Thus, sample 2058 was estimated to be $Cu_{12.73}Fe_{0.53}As_4S_{13}$, sample 2057, to be $Cu_{11.53}Fe_{1.05}As_4S_{13}$, and sample 2059, to be $Cu_{10.98}Fe_{1.5}As_4S_{13}$. Assuming that Cu^+ only is present, these formulae indicate an average valence of iron as 2.40+, 2.35+ and 2.02+, respectively, the first two being in fair agreement with the results of the calculation performed further below, using the equation of Goodenough & Fatseas (1982) to determine the valence of iron from Mössbauer data. Our compositional estimates are also in fair agreement with those of Bortnikov & Nekrasov (1987), who unfortunately indicated their composition fields only graphically. The principal differences with their findings seem to be that (1) they seem not to have reached the compositions richest in Cu at the levels of 0.0 and 0.5 Fe *apfu*, and (2) they interpreted the phase compositions at 1.5 and 2.0 Fe *apfu* as being nonstoichiometric.

The positions of the analyzed phases in the composition space $Cu_{12}As_4S_{13}$ – $Cu_{14}As_4S_{13}$ – $Cu_{10}Fe_2As_4S_{13}$ are indicated in Figure 1, together with their *a* values. Two-thirds of the samples contain no detectable impurities or only traces of a Fe-free phase, luzonite. The remaining samples contain small amounts of dispersed chalcopyrite, bornite or low-Fe digenite; only in three cases (marked by asterisks in Fig. 1) do minor phases reach or exceed 10 vol.% of the charge (Table 1). Persistent problems of this kind were already noticed by Tatsuka & Morimoto (1977) and Bortnikov & Nekrasov (1987), who interpreted them as a sign of nonstoichiometry of synthetic, high-Fe tetrahedrite or tennantite.

With the exception of charge 2052, weighed out as $Cu_{11.5}Fe_{0.5}As_4S_{13}$, the Mössbauer spectra reveal the presence of three valences of iron: 2+, 3+, and an apreciable amount of intermediate-valence iron in the state 2+ < *n* < 3+ at all levels of substitution (Table 2). The ratio of different valences in the spectra observed varies. Relative amounts of Fe^{2+} and Fe^{3+} show opposing trends, whereas the intermediate-valence iron, Fe^{n+}, is most abundant in the broad region around one Fe *apfu* (Fig. 2). The trends of Fe^{2+} and Fe^{3+} contents *versus* total Fe are not linear, reflecting the changing proportions of the intermediate-valence iron in the structure. For Cu-poor charges, it is the Fe^{3+} trend that is closest to linearity, whereas for the Cu-rich charges, it is the Fe^{2+} trend (Fig. 2).

TABLE 2. MÖSSBAUER DATA FOR SYNTHETIC Fe-SUBSTITUTED TENNANTITE

Sample	Component χ-square		Hyperfine parameters				G & F (1982)
			Isomer shift	FHWB	% of total Fe area	Quadrupole splitting	
2052	1	Fe^{3+}	0.34	0.27	100.0	0.28	2.68
	0.335						2.68
2054	1	Fe^{2+}	0.53	0.28 (F)	11.7	2.22	2.29
	2	Fe^{3+}	0.35	0.34	57.4	0.29	2.66
	3	Fe^{n+}	0.49	0.70 (F)	30.9	1.30	2.38
	0.351						2.53
2055	1	Fe^{2+}	0.59	0.34	33.0	2.35	2.18
	2	Fe^{3+}	0.35	0.34	30.8	0.27	2.67
	3	Fe^{n+}	0.45	0.73	36.1	1.41	2.46
	0.385						2.43
2056	1	Fe^{2+}	0.59	0.32	56.2	2.49	2.17
	2	Fe^{3+}	0.36	0.30 (F)	7.6	0.19	2.65
	3	Fe^{n+}	0.52	0.82	36.2	1.55	2.32
	0.409						2.26
2057	1	Fe^{2+}	0.60	0.35	40.0	2.37	2.16
	2	Fe^{3+}	0.37	0.30 (F)	15.5	0.26	2.62
	3	Fe^{n+}	0.57	0.91	44.4	1.45	2.22
	0.404						2.26
2058	1	Fe^{2+}	0.57	0.34 (F)	12.2	2.16	2.23
	2	Fe^{3+}	0.34	0.37	60	0.22	2.69
	3	Fe^{n+}	0.48	0.70 (F)	27.8	1.39	2.40
	0.34						2.55
2059	1	Fe^{2+}	0.58	0.39	52.8	2.40	2.20
	2	Fe^{3+}	0.37	0.34 (F)	18.2	0.30	2.62
	3	Fe^{n+}	0.47	0.74	29.0	1.38	2.42
	0.432						2.34

G & F (1982): Goodenough & Fatseas (1982), valence of Fe and average valence of Fe.

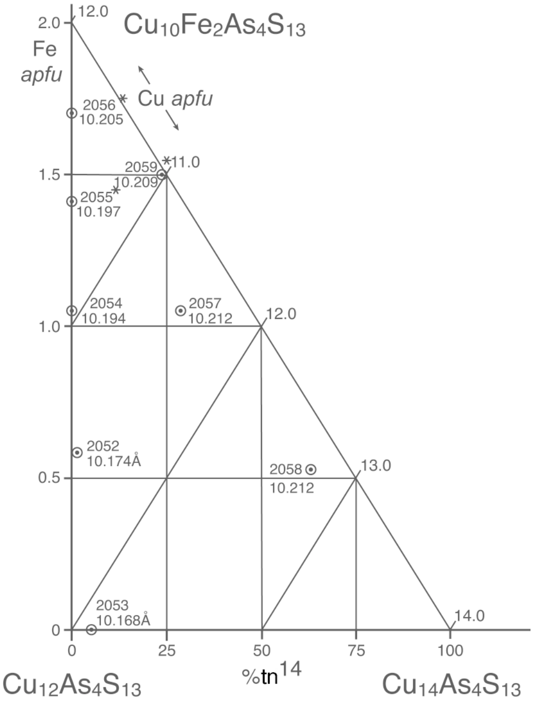

FIG. 1. Position of tennantite samples analyzed by Mössbauer spectroscopy in terms of the composition space $Cu_{12}As_4S_{13}$ – $Cu_{14}As_4S_{13}$ – $Cu_{10}Fe_2As_4S_{13}$. Charge numbers and values of the unit-cell parameter *a* are indicated. The variable % tn^{14} (vertical lines) indicates the percentage of the $Cu_{14}As_4S_{13}$ end-member in the above combination of three end-members.

In spite of varying proportions of Fe species in the samples, the isomer shift of Fe^{3+} changes little with increasing incorporation of Fe. The only exceptions are two Cu-rich samples (2057 and 2059) with only 16–18% of Fe^{3+} evident in the spectrum, for which IS reaches the value of 0.370, known from spectra of bornite (Vaughan & Burns 1972). Similarly, a small decrease in the isomer shift of Fe^{2+} is bound to its minor element content, only 12% in the Cu-poor sample at the level of 0.5 Fe *apfu*. The only significant deviation in the isomer shift of mixed-valence iron from its average values occurs in the sample with the poorest fit.

Quadrupole splitting of Fe^{3+} is fairly constant for all Cu-poor samples with a sufficient percentage of Fe^{3+}; values for Cu-rich samples show evidence of a strong increase with the level of Fe incorporation. It generally increases for Fe^{2+} with increasing amount of incorporated Fe. Trends similar to those of Fe^{2+} are also observed for the mixed-valence iron.

The Mössbauer spectrum of tennantite samples 2052 ($Cu_{11.44}Fe_{0.58}As_4S_{13}$; Fig. 3, Table 1) and 2058 ($Cu_{12.97}Fe_{0.53}As_4S_{13}$), *i.e.*, of those samples with the lowest levels of Fe incorporation, is dominated by doublets of Fe^{3+} with an isomer shift (Table 2) markedly similar to IS = 0.33 measured for $Cu_{11.5}Fe_{0.5}Sb_4S_{13}$ (Makovicky *et al.* 1990). For sample 2052, the quadrupole splitting also is close to 0.269, the value observed in $Cu_{11.5}Fe_{0.5}Sb_4S_{13}$. For $Cu_{12.97}Fe_{0.53}As_4S_{13}$ (sample 2058), this peak is accompanied by a first indication of mixed-valence iron, which amounts to 28% of the peak area. On the following level of iron incorporation, with 1 Fe *apfu*, two charges of pure tennantite display both Fe^{3+} and Fe^{2+} as well as substantial portions of mixed-valence iron (Fig. 4, Table 2). For Fe^{3+}, the quadrupole splitting (QS) values are slightly higher than for the samples with 0.5 Fe *apfu*. For Fe^{2+}, those values are considerably lower than the corresponding values (2.66–2.90) for Fe^{2+} in synthetic tetrahedrite. For the Cu-rich portion of the field, the intermediate-valence iron is the principal form of iron, exceeding the contents of Fe^{2+}, and especially those of Fe^{3+} (Table 2). For the corresponding sample of tetrahedrite, FeT3 ($Cu_{11.07}Fe_{1.01}Sb_4S_{13}$), the Mössbauer spectrum indicates pure Fe^{3+} with a QS value of 0.291, higher than in tennantite; the latter shows a QS value in the range 0.255–0.289.

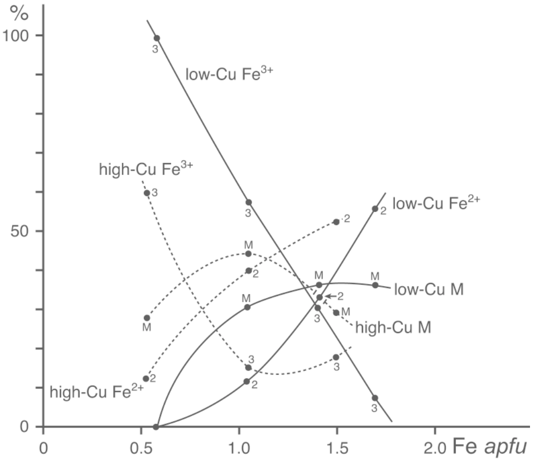

FIG. 2. Trends for Fe^{2+}, Fe^{3+}, and intermediate iron (M) contents *versus* total iron for synthetic tennantite. Trends along the join $Cu_{12}As_4S_{13}$ – $Cu_{10}Fe_2As_4S_{13}$ are visualized using continuous lines, those along the join $Cu_{14}As_4S_{13}$ – $Cu_{10}Fe_2As_4S_{13}$, using stippled lines.

At the level of about 1.5 Fe *apfu*, the proportion of Fe^{2+} exceeds that of Fe^{3+} in the sample 2055 ($Cu_{10.59}Fe_{1.41}Sb_4S_{13}$) (Fig. 5) and especially in sample 2059 ($Cu_{\leq 11.0}Fe_{1.50}Sb_4S_{13}$) (Table 1). Amounts of intermediate-valence iron are significant, this being the principal form of iron in sample 2055 (Table 2). The composition of tennantite with the highest Fe content synthesized in this study is $Cu_{10.30}Fe_{1.70}Sb_4S_{13}$ (sample 2056, Table 1), with a Fe^{2+}:Fe^{3+} ratio equal to 88:12 and a still appreciable content of intermediate-valence iron (36% of total Fe, Fig. 6, Table 2).

DISCUSSION

Synthetic Fe-bearing tennantite differs from the synthetic Fe-bearing tetrahedrite (Charnock *et al.* 1989a, b, Makovicky *et al.* 1990) by the "earlier" appearance of Fe^{2+}, already at the level of 1.0 atoms of Fe (or even at the level of 0.5 atoms of Fe for Cu-rich charges) in a formula unit. In tetrahedrite, Fe^{2+} was not detected for $Cu_{11}Fe_1Sb_4S_{13}$, but only in compositions with Fe exceeding 1 *apfu*, together with mixed-valence iron. Mixed-valence iron represents a substantial portion of total iron in tennantite at room temperature. It is the principal form of iron at the 1.5 Fe *apfu* level of Cu-poor tennantite and at the 1 Fe *apfu* level of Cu-rich tennantite. Its amount is even substantial at the 0.5 Fe *apfu* level of the Cu-rich tennantite, although it is absent at this level in Cu-poor tennantite. Extrapolation of known data-points indicates that intermediate-valence iron is present in the majority of compositions in the solid-solution range of iron-containing tennantite, wherever both Fe^{2+} and Fe^{3+} are present in the solid solution.

The difference in the valence of iron at different stages of substitution between synthetic tennantite and tetrahedrite in which only copper and iron are combined (Makovicky *et al.* 1990) may be due to (a) steric factors and (b) electronic processes.

In tennantite, the Fe–Cu pair may be partly forced into a Fe^{2+}–Cu^{2+} configuration (instead of the Fe^{3+}–Cu^+ configuration) by the necessity for the iron to occupy smaller coordination polyhedra, adjusted to the smaller AsS_3 pyramids. According to Makovicky & Karup-Møller (1994), the radius of Cu^{2+} in tetrahedral coordi-

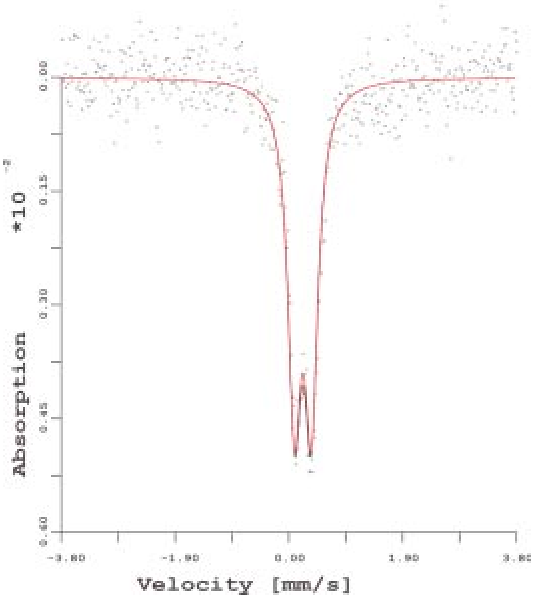

FIG. 3. Mössbauer spectrum of tennantite sample 2052 ($Cu_{11.44}Fe_{0.58}As_4S_{13}$). Red and final fit curves: Fe^{3+}.

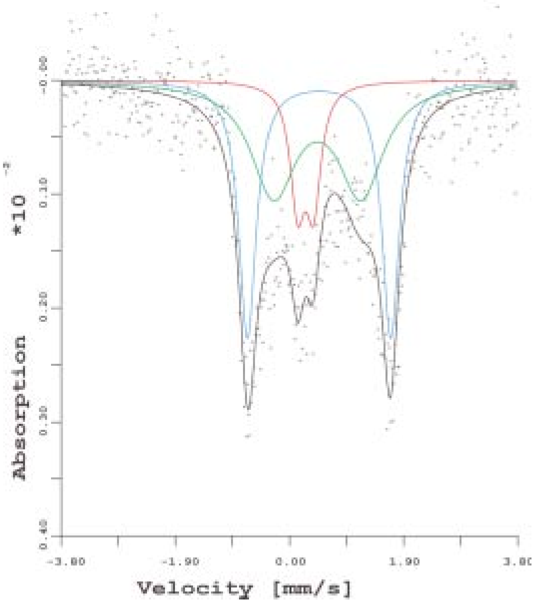

FIG. 4. Mössbauer spectrum of tennantite sample 2057 ($Cu_{11.53}Fe_{1.05}As_4S_{13}$). The Fe^{3+} curve is shown in red, Fe^{2+} curve in blue, mixed-iron curve in green, and the curve describing the overall fit in black.

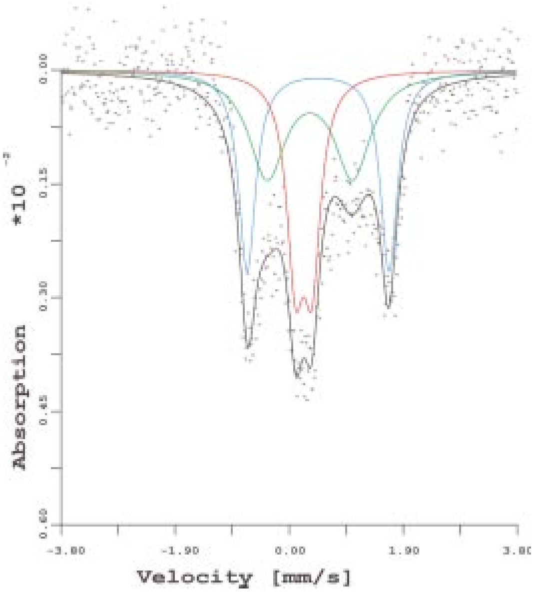

FIG. 5. Mössbauer spectrum of tennantite sample 2055 ($Cu_{10.59}Fe_{1.41}Sb_4S_{13}$).

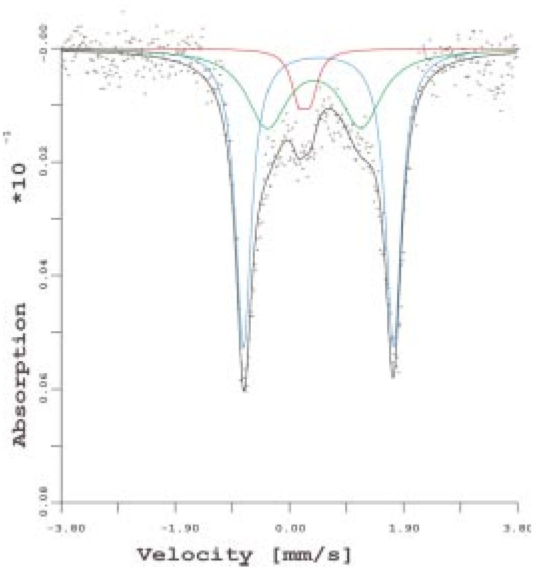

FIG. 6. Mössbauer spectrum of tennantite sample 2056 ($Cu_{10.30}Fe_{1.70}Sb_4S_{13}$).

nation is about 0.50 Å, whereas Shannon (1981) gave r(Cu^+) = 0.635 Å for the same coordination state. Shannon's radius for tetrahedrally coordinated Fe^{2+}(HS) is 0.66 Å, and for Fe^{3+}, it is 0.555 Å. Therefore, the combination of Fe^{2+} and Cu^{2+} has a sum of radii 2–3% lower than the combination Fe^{3+}–Cu^+. Additional factors that determine this partial conversion may be different ionization potentials and electronegativities for As^{3+} and Sb^{3+} (Emsley 1994). Arsenic, with its distinctly higher ionization potential and electronegativity than Sb, might attract a portion of electrons from S, forcing in turn Fe and Cu into their higher oxidation states. The ionization energy for $Cu^+ \rightarrow Cu^{2+}$ being lower than that for $Fe^{2+} \rightarrow Fe^{3+}$ (Emsley 1994), electrons would be preferably drawn from Cu and the Cu^{2+} state would be favored, giving the same resulting balance of valences as the action of geometrical constraints.

In no case does the IS (Fe^{3+}) value observed in synthetic tennantite approach the IS value known for chalcopyrite (0.23 mm/s: Greenwood & Whitfield 1968). Only for samples 2057 and 2058, the richest in Cu, is IS equal to the value observed for bornite (0.37 mm/s: Vaughan & Burns 1972). The majority of synthetic tennantite samples with between 0.5 to ~1.5 Fe atoms in a formula unit have a value of IS in the narrow range 0.342–0.349. The IS values for Fe^{2+} remain in the range 0.533–0.601. The former values are very close to the isomer shift of Fe^{3+} in "amorphous Fe_2S_3" (IS = 0.35 ± 0.06 mm) observed by Stiller *et al.* (1978) and to the isomer shift of tetrahedrally coordinated Fe^{3+} in $(Pb_2FeS_3)_{0.58}NbS_2$ (IS = 0.30 mm) observed by Moëlo *et al.* (1997) and to that in $[Sr(Fe,Nb)_{0.5}S_{1.5}]_{1.13}NbS_2$ (IS = 0.32 mm/s) investigated by Leynaud *et al.* (2002). For comparison, values of IS for octahedrally coordinated Fe^{3+} are quoted as 0.46–0.50 mm (Ben Salem *et al.* 1988).

A tentative explanation of the observed IS values can be formulated on the basis of conclusions reached by Goodenough & Fatseas (1982). They based their conclusions on an extensive review of Mössbauer results from iron-bearing sulfides, and found that IS is not only a sensitive function of formal valence of the iron (number of *3d* electrons per iron atom), of (high *versus* low) spin state, but also of electron delocalization and of a net charge-transfer in the course of Fe – anion – transition metal superexchange interactions. Despite a marked change in IS with electronegativity of the ligand, for a given ligand (single S in our case), valence of iron and ligand coordination, the range of IS values is narrow. Increased covalency reduces IS, which can be seen as minor shifts in IS (in the second decimal) when the increased (decreased) electropositive character of the counterion forces increase (decrease) of the covalent character of the Fe–S bond.

Under the assumption that the magnitude of IS varies linearly with the valence state (the formal valence-state modified by net transfer from superexchange interactions, electron delocalization or both), Goodenough & Fatseas (1982) chose 0.18 mm/s and 0.68 mm/s as typical (average), unmodified values for high-spin Fe^{3+} and Fe^{2+} in tetrahedral coordination with sulfur. This proposal leads to the relation

$$\mathrm{IS}(Fe^{m+}) = 1.68 - 0.5\ m$$

where $m+$ is the formal (mean where applicable) valence of iron.

The resulting effective valences for synthetic Fe-bearing tennantite (Table 2) depend strongly on the validity of the choice of "standard states" by Goodenough & Fatseas; these might be regarded in light of the above-quoted values from layered misfit sulfides as tentative. For Fe^{2+}, the effective valences range from about $Fe^{2.17–2.16+}$ for Fe-rich samples to $Fe^{2.29+}$ for the Cu- and Fe-poor sample 2054 at the 0.5 Fe *apfu* level. The effective valence of Fe^{3+} lies between $Fe^{2.68–2.69+}$ for the 0.5 Fe *apfu* level and $Fe^{2.62–2.65+}$ for the samples richest in Fe, perhaps an excessively low estimate.

Comparison of the average valence of iron obtained from the equation of Fatseas & Goodenough (Table 2) with the results of simple calculations based on the chemical formulae of Cu-poor phases indicates very similar results for the samples with more Fe than 1 *apfu.* It proves again that the simple model of Fe^{3+} as the only type of iron present in the compositions with Fe ≤ 1 *apfu*, valid for tetrahedrite (Makovicky *et al.* 1990), is not valid for tennantite. For Cu-rich compositions, the average valence of iron confirms that their true composition has moved away from the join $Cu_{14}Sb_{11}S_{13}$ – $Cu_{10}Fe_2Sb_4S_{13}$ toward compositions poorer in Cu, as suggested above.

If the postulates of Goodenough & Fatseas (1982) are applied to the crystal structure of tennantite, the differences between the formal and the effective charges of the two valence states of iron can be attributed primarily to the net transfer of charge due to superexchange (*via* S) involving Fe and Cu in corner-sharing tetrahedra, with rarer instances of such Fe–Fe pairs. Electron delocalization should play a decisive role in the phenomenon analyzed further below. It is aided by the more substantial overlap of electron orbitals in the tennantite structure because of shorter interatomic distances in tennantite than in tetrahedrite.

Formally divalent Cu still plays a role in sample 2054 (0.44 Cu^{2+} per ideal formula unit with the observed iron valences), as it does in the corresponding tetrahedrite $Cu_{11}Fe_1Sb_4S_{13}$ (Makovicky *et al.* 1990), for which the IS value gives $Fe^{2.73+}$, resulting in 0.27 Cu^{2+} per ideal formula unit. Without the superexchange charge-transfer, only trivalent Fe and univalent copper should be present. Ease of superexchange charge-transfer (and, perhaps, also of direct metal–metal electron transfer involving small amounts of interstitial copper: see Makovicky & Skinner 1979) can be seen from the lack of localization of the two excess positive charges, which can be formally ascribed to the array of copper atoms in unsubstituted tetrahedrite $Cu_{\sim 12.3}Sb_4S_{13}$ (Makovicky & Skinner 1979).

The presence of Fe^{2+} in tennantite is accompanied by the appearance of *intermediate-valence iron* in a Mössbauer spectrum. In all spectra except for sample 2052 at 0.5 Fe *apfu* and sample 2056 at ~1.5 Fe *apfu*, both "Fe^{2+}" and "Fe^{3+}" are present in substantial amounts (≥10% of total Fe peak area), whereas the percentage of intermediate-valence iron ranges from moderate to substantial (28–44%). Although it appears that in tetrahedrite the bulk of the iron is in well-defined valence states and does not take part in Fe–Fe electron transfer (Charnock *et al.* 1989a, b, Makovicky *et al.* 1990), between one-quarter and one-half of all the Fe is involved in this transfer in tennantite.

The doublets of intermediate-valence iron have peaks broader than are those of Fe^{3+} and Fe^{2+} (Table 2). The reasons may be twofold: (1) they represent a composite of several Mössbauer doublets originating in electron transfers between pairs of Fe atoms in various mutual configurations (various environments), with or without intervening Cu, or (2) the exchange frequency between Fe^{2+} and Fe^{3+} exceeds only slightly the inverse lifetime of an excited Fe nucleus at the temperature of measurements. Both factors may combine; the frequency of exchange may also be modified by structural equivalence or non-equivalence of the two sites involved.

Such considerations were put forward for electron exchange in oxide spinels by Lotgering & van Diepen (1977) and for $(Mg,Fe)SiO_3$ perovskite by Fei *et al.* (1994). In the case of both synthetic tennantite and tetrahedrite, the situation is complicated by the low concentration of iron, 0.5 to 2 Fe atoms in each six-fold ring of tetrahedra around an AsS_3 (or SbS_3) pyramid. Four such six-fold rings join around tetrahedral cavities.

For the tetrahedrally coordinated metal sites, no short Fe–Fe contacts exist in the structure of tennantite, owing to a lack of common edges between adjacent tetrahedra. Therefore, superexchange *via* common S^{2-} anions and, eventually, intervening Cu atoms has to be postulated as a probable mechanism of electron transfer. The role of small amounts of mobile Cu, potentially present in these structures (*cf.* Makovicky & Skinner 1978, 1979) might also be important in this charge transfer. The intervention of Cu appears likely: mixing of the Cu *s*, *d* band with the Fe *d* band and S *p* conduction band in $CuFeS_2$ has been deduced from *L*-edge X-ray absorption spectra by Grioni *et al.* (1989) and Pattrick *et al.* (1993).

Alternatively, in the interpretation of Charnock *et al.* (1989a, b), 0.5 to 2 Fe atoms might occur in a cluster of 6 Cu atoms in triangular coordination [denoted as the Cu(2) sites in the structures of tetrahedrite–tennantite: Johnson *et al.* (1988)] within each of the large tetrahedral cavities. The IS values of Fe^{3+}, expected for such interpretation, would be much lower than the observed ones, and thus this hypothesis can be excluded for tennantite.

Changes in the intensity of the electron exchange processes with temperature remain to be investigated. If the electron delocalization is thermally activated (Lotgering & van Diepen 1977), the proportion of intermediate-valence iron and the sharpness of its doublet peaks are expected to increase with temperature, as shown for ilvaite by Evans & Amthauer (1989), for example. Eventually, the full disappearance of Fe^{2+} and Fe^{3+} peaks could be reached, a stage described in the case of Cu–Fe rhodium and chromium thiospinels by Riedel *et al.* (1981). In the latter work, broad peaks of intermediate-valence iron were interpreted as an example of an overlap of multiple peaks, reflecting several distinct environments of iron.

The model proposed here gives a plausible explanation to the observed Mössbauer characteristics of iron in synthetic tennantite in terms of fractional valences due to the net effects of superexchange charge-transfer. The values of Fe valence obtained from the measured IS values depend crucially on the validity of the equation of Goodenough & Fatseas (1982). This phenomenon places tennantite (and tetrahedrite) into a group of sulfides in which, owing to the band structure, appreciable differences between formal and effective charges occur for iron, alongside such compounds as Cu_2FeSnS_4 (Eibschutz *et al.* 1967), thalcusite $Tl_2Cu_3FeS_4$ (Forcher *et al.* 1988), bornite (Townsend *et al.* 1977) and $FeCr_2S_4$ (Brossard *et al.* 1980), as opposed to compounds such as stoichiometric chalcopyrite (Greenwood & Whitfield 1968), for which no appreciable deviations from formal charge are claimed. In addition, the electron-transfer phenomenon resulting in broad peaks of "intermediate-valence iron" and the IS values for "Fe^{3+}" make the situation in tennantite similar to that in the copper-bearing thiospinels investigated by Riedel *et al.* (1981).

ACKNOWLEDGEMENTS

Assistance of Mr. H. Singh during the sample preparation and of Mrs. C. Sarantaris and Mrs. Brita Munch in preparation of the manuscript are gratefully acknowledged. We profited from thorough reviews by Dr. Y. Moëlo (Nantes), an unknown referee, as well as by kind improvements by Associate Editor F.F. Foit Jr. and R.F. Martin.

REFERENCES

BEN SALEM, A., FATSEAS, G., MOLINIÉ, P. & MEERSCHAUT, A. (1988): Electronic transfer intercalation processes: transfer and localization in $Li_yFe_{1.33}Nb_{2.67}Se_{10}$. *Synth. Met.* **25**, 207-225.

BORTNIKOV, N.S. & NEKRASOV, I.YA. (1987): Composition and phase relationships of tennantite in the system Cu–Fe–As–S at 500°C. *Dokl. Akad. Nauk SSSR* **297**, 449-452 (in Russ.).

BROSSARD, L., GOLDSTEIN, L., GIBART, P. & DORMAN, J.-L. (1980): Non-affinity of Fe^{2+} for B sites in iron thiochromites and compared band structures of oxide and sulfide spinels. *J. Phys. Chem. Solids* **41**, 669-678.

CHARLAT, M. & LÉVY, C. (1975): Influence des principales substitutions sur le paramètre cristallin dans la série tennantite–tétrahedrite. *Bull. Soc. fr. Minéral. Cristallogr.* **98**, 152-158.

CHARNOCK, J.M., GARNER, C.D., PATTRICK, R.A.D. & VAUGHAN, D.J. (1989a): EXAFS and Mössbauer spectroscopic study of Fe-bearing tetrahedrites. *Mineral. Mag.* **53**, 193-199.

________, ________, ________ & ________ (1989b): Coordination sites of metals in tetrahedrite minerals determined by EXAFS. *J. Solid State Chem.* **82**, 279-289.

EIBSCHUTZ, M., HERMAN, E. & STRICKMAN, S. (1967): Determination of cation valencies in $Cu_2{}^{57}Fe^{119}SnS_4$ by Mössbauer effect and magnetic susceptibility measurements. *J. Phys. Chem. Solids* **28**, 1633-1636.

EMSLEY, J. (1994): *The Elements* (2nd ed.). Clarendon Press, Oxford, U.K.

EVANS, B.J. & AMTHAUER, G. (1980): The electronic structure of ilvaite and the pressure and temperature dependence of its ^{57}Fe Mössbauer spectrum. *J. Phys. Chem. Solids* **41**, 985-1001.

FEI, Y., VIRGO, D., MYSEN, B.O., WANG, Y. & MAO, H.K. (1994): Temperature-dependent electron delocalization in (Mg,Fe) SiO_3 perovskite. *Am. Mineral.* **79**, 826-837.

FORCHER, K., LOTTERMOSER, W. & AMTHAUER, G. (1988): Mössbauer study of raguinite, $TlFeS_2$, and thalcusite, $Cu_3Tl_2FeS_4$. *Neues Jahrb. Mineral., Abh.* **160**, 25-28.

GOODENOUGH, J.B. & FATSEAS, G.A. (1982): Mössbauer ^{57}Fe isomer shift as a measure of valence in mixed-valence sulfides. *J. Solid State Chem.* **41**, 1-22.

GREENWOOD, N.N. & WHITFIELD, H.J. (1968): Mössbauer effect studies on cubanite ($CuFe_2S_3$) and related iron sulphides. *J. Chem. Soc.* (**A**), 1697-1699.

GRIONI, M., GEODKOOP, J.B., SCHOORL, R., DE GROT, F.M.F., FUGGLE, J.C., SCHÄFERS, F., KOCH, E.E., ROSSI, G., ESTEVA, J.-M. & KARNATAK, R.C. (1989): Studies of copper valence states with Cu L_3 x-ray absorption spectroscopy. *Phys. Rev.* **B 39**, 1541-1545.

JOHNSON, N.E., CRAIG, J.R. & RIMSTIDT, J.D. (1988): Crystal chemistry of tetrahedrite. *Am. Mineral.* **73**, 389-397.

KAWAI, S., ITO, Y. & KIRIYAMA, R. (1972): Magnetic susceptibility, Mössbauer effect and conductivity in sphalerite and tetrahedrite. *J. Mineral. Soc. Japan* **10**, 487-498 (in Japanese).

LEYNAUD, O., LAFOND, A., MOËLO, Y., PALVADEAU, P. & MEERSCHAUT, A. (2002): Crystal structures and magnetic properties of the two misfit layer compounds: $[SrGd_{0.5}S_{1.5}]_{1.16}NbS_2$ and $[Sr(Fe,Nb)_{0.5}S_{1.5}]_{1.13}NbS_2$. *J. Solid State Chem.* **168**, 41-51.

LIND, I.L. & MAKOVICKY, E. (1982): Phase relations in the system Cu–Sb–S at 200°C, 10^8 Pa by hydrothermal synthesis. Microprobe analysis of tetrahedrite – a warning. *Neues Jahrb. Mineral., Abh.* **145**, 134-156.

LOTGERING, F.K. & VAN DIEPEN, A.M. (1977): Electron exchange between Fe^{2+} and Fe^{3+} ions on octahedral sites in spinels by means of paramagnetic Mössbauer spectrum and susceptibility measurements. *J. Phys. Chem. Solids* **38**, 565-572.

LOTTERMOSER, W., FORCHER, K. & AMTHAUER, G. (1993): Fe, Ti ordering in acentric neptunite: measurements with Mössbauer spectroscopy. *Terra Abstr. Suppl.* **1**, 494.

MAKOVICKY, E., FORCHER, K., LOTTERMOSER, W. & AMTHAUER, G. (1990): The role of Fe^{2+} and Fe^{3+} in synthetic Fe-substituted tetrahedrite. *Mineral. Petrol.* **43**, 73-81.

________ & KARUP-MØLLER, S. (1994): Exploratory studies on substitution of minor elements in synthetic tetrahedrite. I. Substitution by Fe, Zn, Co, Ni, Mn, Cr, V and Pb. Unit cell parameter changes on substitution and the structural role of "Cu^{2+}". *Neues Jahrb. Mineral., Abh.* **167**, 89-123.

________ & SKINNER, B.J. (1978): Studies of the sulfosalts of copper. VI. Low-temperature exsolution in synthetic tetrahedrite solid solution, $Cu_{12+x}Sb_{4+y}S_{13}$. *Can. Mineral.* **16**, 611-623.

________ & ________ (1979): Studies of the sulfosalts of copper. VII. Crystal structures of the exsolution products $Cu_{12.3}Sb_4S_{13}$ and $Cu_{13.8}Sb_4S_{13}$ of unsubstituted synthetic tetrahedrite. *Can. Mineral.* **17**, 619-634.

MASKE, S. & SKINNER, B.J. (1971): Studies of the sulphosalts of copper. I. Phases and phase relations in the system Cu–As–S. *Econ. Geol.* **66**, 901-918.

MOËLO, Y., LAFOND, A., DENDON, C., COULON, N., LANCIN, M. & MEERSCHAUT, A. (1997): $(Pb_2FeS_3)_{0.58}NbS_2$. *C.R. Acad. Sci. Paris, Sér. IIb* **325**, 287-296.

MOZGOVA, N.N. & TSEPIN, A.I. (1983): *Tetrahedrite–Tennantite Series*. Nauka, Moscow, Russia (in Russ.).

PATTRICK, R.A.D., VAN DER LAAN, G., VAUGHAN, D.J. & HENDERSON, C.M.B. (1993): Oxidation state and electronic configuration determination of copper in tetrahedrite group minerals by L-edge x-ray absorption spectroscopy. *Phys. Chem. Minerals* **20**, 395-401.

RIEDEL, E., KARL, R. & RACKWITZ, R. (1981): Mössbauer studies of thiospinels. V. The systems $Cu_{1-x}Fe_xMe_2S_4$ (Me = Cr,Rh) and $Cu_{1-x}Fe_xCr_2(S_{0.7}Se_{0.3})_4$. *J. Solid State Chem.* **40**, 255-265.

SHANNON, R.D. (1981): Bond distances in sulfides and a preliminary table of sulfide crystal radii. *In* Structure and Bonding in Crystals II (M. O'Keeffe & A. Navrotsky, eds). Academic Press, New York, N.Y. (53-70).

STILLER, A.H., MCCORMICK, B.J., RUSSELL, P. & MONTANO, P.A. (1978): Existence and stability of a simple sulfide of iron (III). *J. Am. Chem. Soc.* **100**, 2553-2554.

TATSUKA, K. & MORIMOTO, N. (1977): Tetrahedrite stability relations in the Cu–Fe–Sb–S system. *Econ. Geol.* **72**, 258-270.

TOWNSEND, M.G., GOSSELIN, J.R., TREMBLAY, R.J., RIPLEY, L.G., CARSON, D.W. & MUIR, W.B. (1977): A magnetic and Mössbauer study of magnetic ordering and vacancy clustering in Cu_5FeS_4. *J. Phys. Chem. Solids* **38**, 1153-1159.

VAUGHAN, D.J. & BURNS, R.G. (1972): Mössbauer spectroscopy and bonding in sulphide minerals containing four-coordinated iron. *24th Int. Geol. Congress* (*Montreal*), *Sect.* **14**, 158-167.

Received December 8, 2002, revised manuscript accepted August 20, 2003.